Investigating the Pore Structure Characteristics and Reservoir Capacities of Lower Jurassic Continental Shale Reservoirs in the Northeastern Sichuan Basin, China

Tao Jiang[1,2,3]*, Zhijun Jin[2,3,4], Guangxiang Liu[2,3], Zongquan Hu[2,3], Xuanhua Chen[1], Zhongbao Liu[2,3] and Guanping Wang[5]

[1]Chinese Academy of Geological Sciences, Beijing, China, [2]State Key Laboratory of Shale Oil and Gas Enrichment Mechanisms and Effective Development, Beijing, China, [3]Petroleum Exploration and Production Research Institute, SINOPEC, Beijing, China, [4]Institute of Energy, Peking University, Beijing, China, [5]China University of Geosciences (Beijing) Energy Institute, Beijing, China

The Lower Jurassic shale in the northeastern Sichuan Basin is one of the main research intervals of continental shale gas. The shale pore structure is an important indicator for evaluating the reservoir capacities of shale reservoirs. We concentrate on the pore structure to indicate reservoir capacity using several testing methods, for example, N_2 adsorption-high-pressure mercury pore size combined experiments, X-ray diffraction (XRD) experiments, and the total organic carbon (TOC) method. The results show that the clay mineral content of the continental shale is high. The pore type is mainly a mineral matrix pore, followed by an organic matter pore, and the microcracks are locally developed; the distribution interval of the main pore size is mesoporous, between 10 and 50 nm; the pore volumes and specific surface areas of the continental shale reservoirs are negatively correlated or unrelated to the TOC, mainly due to the failure of pore development in the organic vitrinite and fusinite and the occupation of pore volume and adsorption sites by the soluble organic matter. The larger pores are mainly formed by clay minerals; the reservoir capacities of the continental shale reservoirs were evaluated using a two-factor evaluation method of the pore volume and specific surface area. It was found that the continental shale mainly comprises free reservoirs and has a storage gas capability level of II–IV. The research results elucidate the pore structure characteristics and reservoir capacities of the continental shale reservoirs in the northeastern Sichuan Basin, having important theoretical and guiding significance for the gas-bearing evaluation and dessert target optimization of the continental shale in the study area.

Keywords: northeastern Sichuan Basin, lower Jurassic, continental shale reservoirs, pore structure characteristics, reservoir capacity

INTRODUCTION

Shale gas is mainly found in dark shale or carbonaceous mudstone formations, which have adsorbed, free, and dissolved states and exist in thin interlayers, such as sandstone and limestone, inside the shale section. It has the characteristics of low resource abundance, a widely developed area, "self-generation and self-storage," and requires advanced petroleum engineering technology to be commercially exploited (Curtis, 2002; Dong et al., 2016a). With the changes in exploration ideation and development of technology, shale gas exploitation has been a huge success in North America since 2000 (Curtis, 2002; Montgomery et al., 2005; Warlick, 2006). China also has huge reserves of shale gas resources (Dong et al., 2016b; Yang et al., 2017; Zhang et al., 2017). At present, marine shale exploitation has made great breakthroughs in the Sichuan Basin and surrounding areas (Zhu et al., 2012; Liu et al., 2015; Guo et al., 2016; Han et al., 2016; Jin et al., 2016; Nie et al., 2016; Nie et al., 2017a; Liang et al., 2017; Liu et al., 2017; Wu et al., 2018; Wu et al., 2019). Meanwhile, continental shale exploitation has also achieved good test productivity results in the Yanchang Formation of the Ordos Basin and Ziliujing Formation of the Yuanba area of the Sichuan Basin, which has become one of the important replacement fields of oil and gas exploration (Zhu et al., 2012; Qiu et al., 2015; Long et al., 2016).

Shale is a porous medium with a complex pore structure and strong heterogeneity (Chen et al., 2011; Chen et al., 2016; Chen et al., 2017). In recent years, the technical methods of studying pores have been innovated and continuously improved, which has laid a good foundation for the study of shale pore structure. The research methods concerning pore structure can be divided into indirect measurements and direct observations (Chalmers et al., 2012; Yang Feng et al., 2014). The commonly used indirect measurement methods include the high-pressure mercury injection method, gas adsorption method, and nuclear magnetic resonance method (Schmitt et al., 2013; Tian et al., 2013), which are commonly used to quantitatively characterize the micro-/nanopores of shale and their storage capacity. Direct observation methods include casting thin-section observation, scanning electron microscope observation, and CT observation. Due to the low resolution of optical microscopy, optical microscope analysis is usually only used to observe conventional micron-scale pores. Therefore, the study of the pore structure in shale with abundant organic matter is mainly conducted by using high-resolution field emission scanning electron microscopy, FIB-SEM, nano-CT, and other equipment to study the different micro/nanopore types and pore connectivities in shale reservoirs (Tang et al., 2015; Wang et al., 2016a; Wang et al., 2016b; Zhang et al., 2022). Because of the differences within the range of various methods of pore diameter characterization, the comprehensive use of various methods can more effectively depict the pore characteristics of shale samples.

The "self-generation and self-storage" characteristics and occurrence state of shale gas determine the factors that should be considered in reservoir evaluation, mainly including the characteristics of organic matter, mineral composition, rock storage space, and rock mechanics properties of gas-bearing shale (Jarvie et al., 2007; Zhang et al., 2011; Zhang et al., 2020a). Research on shale reservoir storage capacity has been carried out in many aspects by scholars, mainly through the establishment of models, adsorption analysis experiments, and other methods to study and evaluate it (Hao et al., 2013; Ji et al., 2016). However, the applicability of these evaluation methods is more limited. The criteria and methods of shale reservoir storage capacity evaluation in different blocks and layers are at the initial stages of research, which restricts the prediction and comparison of shale reservoir storage capacities.

In this study, argon-ion scanning electron microscopy combined with gas adsorption–high-pressure mercury aperture experiments were used to characterize the pore volume, specific surface area, and pore size distribution of continental shale in the Ziliujing Formation in the northeast Sichuan Basin. The reservoir capacities of the study area are evaluated by the factors of pore volume and specific surface area. These research results have important guiding significance for the exploration of continental shale gas in the Sichuan Basin.

GEOLOGICAL BACKGROUND

The northeast Sichuan Basin is in the northern part of the Yangtze Plate, which comprises the areas of the Tongnanba structural belt of the northern Sichuan Depression, the gentle structural zone of central Sichuan, and the fold belt of eastern Sichuan in the Sichuan Basin (**Figure 1**). The Yuanba block is located at the northern edge of the Yangtze Plate and is adjacent to the Qinling fold belt. It is situated in the superimposed block of the Micang Mountains, the arc structural belt of the Daba Mountains, and the arc fold belt of the eastern Sichuan Basin (Zhang et al., 2013; Wei et al., 2014). The Fuling area lies in the arc high and steep structural zones in the eastern Sichuan Basin, which is classified as the Wanxian synclinorium and extends toward the northeast direction (Wang and Wang, 2013). The northeast Sichuan Basin experienced the Caledonian movement, Hercynian movement, and Indo-China movement. During the Jurassic period, due to the disappearance of the Songpan–Ganzi Sea and western sea, it was surrounded and evolved into an inland lake with a river delta (Deng, 1992; Tong, 1992).

The Lower Jurassic Ziliujing Formation in the northeast Sichuan Basin is of unequal thickness, exhibiting the lithologies of lake-phase mud shale and shell limestone. It is divided into four members from bottom to top, including the Zhenzhuchong Member, Dongyuemiao Member, Ma'anshan Member, and Da'anzhai Member, and the contact with the underlying Triassic Xujiahe Formation is unconformable–disconformable and that with the contemporary heterotropical Qianfoya Formation or Lianggaoshan Formation is disconformable. The organic-rich shale is mainly developed in the Dongyuemiao Member of the Fuling area and Da'anzhai Member of the Yuanba block, which are the key exploration areas for continental shale oil and gas (Zhou et al., 2013a; Zhou et al., 2013b; Wang and Wang, 2013; Nie et al., 2017b; **Figures 1B,C**).
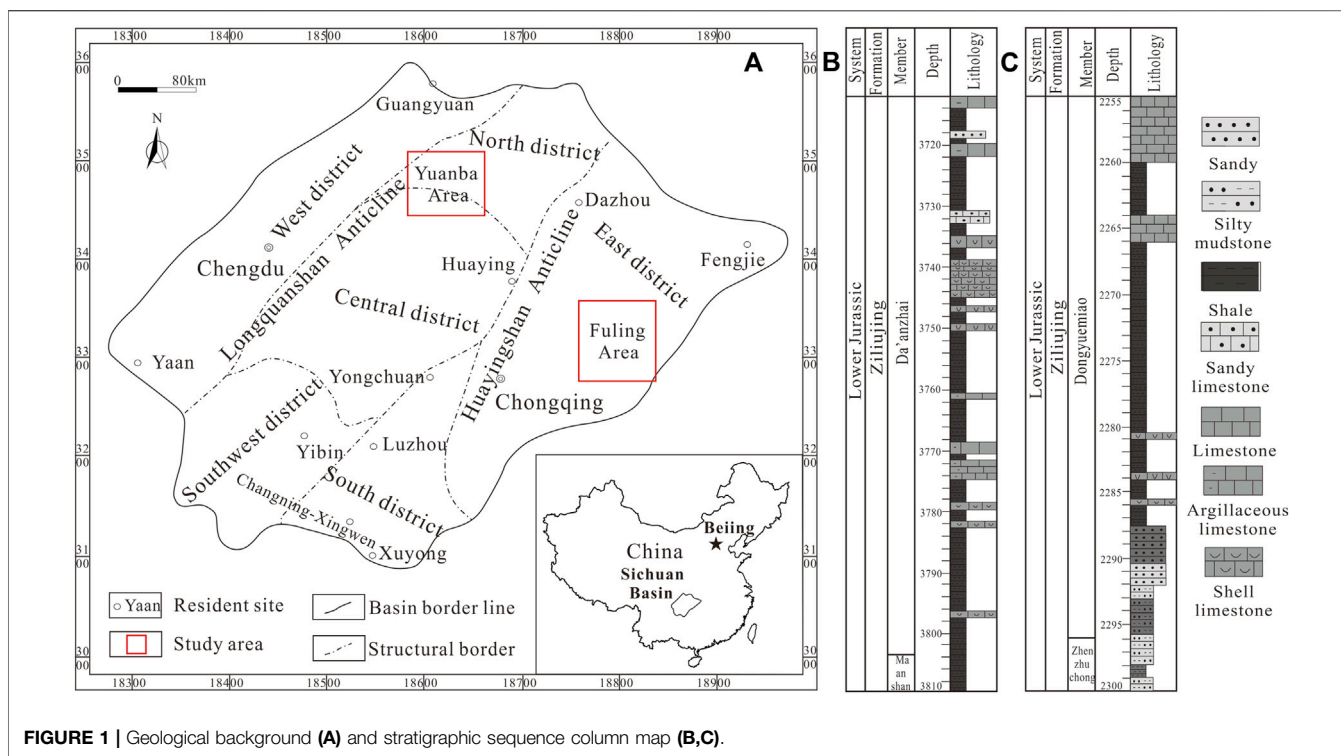
FIGURE 1 | Geological background **(A)** and stratigraphic sequence column map **(B,C)**.

SAMPLING AND EXPERIMENTAL METHODS

Sample Nos. 1–6 are sampled from the XL-101 well of the eastern Fuling area and the FY-1 well of the Dongyuemiao Member. Sample Nos. 7–13 are sampled from the YL-4 well in the Yuanba area of the Da'anzhai Member. The pore structure and rock composites are tested with the following methods: X-ray Diffraction (XRD), N_2 adsorption-high pressure mercury pore size combined experiment, and the total organic carbon (TOC) testing method.

X-Ray Diffraction

The parallel samples were selected, washed to a fluorescence level of 4 or below, dried at temperatures below 60°C, cooled to room temperature, crushed into 1–2 g samples of less than 1 mm with a prototype crusher, and then submerged in an agate mortar to less than 40 microns. A back pressure method is used to prepare the test pieces, and the diffraction intensity of each test surface is measured by using the instrument. The baseline is reasonably selected for qualitative and quantitative analysis. The testing procedure refers to SY/T 5163-2010 (Chinese oil and gas industry standard).

N_2 Adsorption-High Pressure Mercury Pore Size Combined Experiment

The instrument used in this study was a JW-BK222-type instrument manufactured by the Cnpowder Company of China. The instrument has a detection limit of 0.0005 m^2/g for

the specific surface area and 0.0001 ml/g for pore volume. The pressure control interval was less than 0.1 KPa by using a balanced pressure intelligent control method, and the maximum pressure point of adsorption can be automatically controlled. A 1–2 g sample was smashed to 60–80 mesh. A vacuum was applied at 110°C for 14 h, and then a nitrogen isothermal adsorption–desorption experiment was performed under a liquid nitrogen atmosphere (77.4 K), and the procedures were in accordance with the Chinese national standard GB/T21650.2-2008. A multipoint BET model was used to calculate the specific surface area of the pore size distribution, which was obtained by adsorption curves using the BJH model. The MICP was implemented by using an AutoPoreIV9520 capillary pressure curve determinative instrument produced by MICROMERITICS™. The testing range was 3 nm–1000 μm, and the precision was less than ±0.0001 ml. The samples that were tested by NMR were evaluated using AutoPoreIV9520 in accordance with the Chinese national standard GB/T21650.1-2008 after being dried at 60°C for 48 h.

Argon-Ion Polishing Scanning Electron Microscope

The argon-ion polishing scanning electron microscope experiments were conducted in the State Key Laboratory of Shale Oil and Gas Enrichment and Effective Development, Wuxi, Jiangsu.

First, the shale samples are cut into appropriately sized blocks along the vertical bedding direction, and then the shale

TABLE 1 | Total organic carbon (*TOC*), mineralogical composition, and pore structure parameters of shale samples.

Layer sample	No.	Well	Depth (m)	TOC/ %	Ro/ %	Mineral composition/%					BET surface area/(M² g⁻¹)	BJH pore volume/ (Cm³ g⁻¹)
						Quartz	Feldspar	Carbonate	Pyrite	Clay		
The Dongyuemiao Member in Fuling area	1	FY1	2736.3	1.33	1.19	23.1	2.6	12.4	0.4	61.5	1.706	0.0064
	2	XL101	2294.3	0.58	1.05	42.7	9.5	3.8	0.9	43.1	3.251	0.0045
	3	XL101	2275.6	1.97	0.96	20.1	2.6	9.6	0.3	67.4	1.048	0.0072
	4	XL101	2275.5	1.96	0.96	22.3	2.3	18.6	0.7	56.1	1.337	0.0064
	5	XL101	2274.2	1.84	1.02	27.5	2.3	9.5	0.4	60.3	0.772	0.0041
	6	XL101	2269.7	1.46	0.99	23.5	2.8	9.2	0.6	63.9	0.863	0.0057
The Da'anzhai Member in Yuanba area	7	YL4	3790.1	0.88	1.43	33.4	3.0	10.0	0.8	52.8	6.918	0.0136
	8	YL4	3786.5	0.70	1.44	50.3	6.9	3.7	0.3	38.8	4.989	0.0089
	9	YL4	3760.8	1.31	1.38	32.5	3.8	23.0	1.9	38.8	2.206	0.0104
	10	YL4	3755.5	0.79	1.36	29.2	3.1	6.7	2.0	59.0	3.578	0.0117
	11	YL4	3754.4	0.78	1.35	26.4	2.8	6.4	0.9	65.3	4.411	0.0133
	12	YL4	3752.6	1.31	1.31	34.8	3.6	8.4	1.3	51.9	3.323	0.0099
	13	YL4	3748.2	1.23	1.33	28.8	2.0	10.1	1.3	57.8	2.486	0.0112

surfaces are mechanically flattened using a German Leica TXP fine grinder. Finally, the ground shale sheets are added into a German Leica RES102 ion thinner to set appropriate working parameters and bombard the sample surface with argon ions. In this experiment, the working voltage of the argon-ion polishing instrument is set to 5 kV, the electric current is 2.2 mA, and the polishing time is 3–4 h. The polished samples are fixed on the sample table with conductive adhesive.

A layer of gold film was plated on the surface to increase the electrical conductivity and inhibit sample charging before observations with FEI Helios 650. In addition, secondary electrons (SEs) and the backscattered electrons (BSEs) were detected with an accelerating voltage of 2.0 KV, a working distance of 3–4 mm, and an electron beam current of 50 pA–0.2 nA. The different contrast and morphology features were used to empirically distinguish minerals and pores, and the minerals were identified accurately with X-ray energy dispersive spectrometry (EDS) measurements.

RESULTS

Organic Matter and Mineral Composition

The study of marine shale indicates that higher organic matter content (*TOC*) is beneficial to the development of organic matter pores and provides vital storage space for shale gas (Ji et al., 2014; Tang et al., 2015; Ji et al., 2016; Tang et al., 2016; Tang et al., 2017). When the organic matter begins to evolve into oil and gas ($R_o > 0.60\%$), organic matter pores start to develop, and when the liquid hydrocarbon and kerogen cracking phase proceeds, organic matter pores are generated massively (Reed and Loucks, 2007; Slatt and O'Brien, 2011; Curtis et al., 2012). However, due to the diversity in the sedimentary environment, source material, and deposition rate, the *TOC* and R_o between marine and continental shale are significantly different.

Organic Geochemical Parameters of Continental Shale Reservoirs

The experimental results of the organic matter content (*TOC*), vitrinite reflectance (R_o), and X-ray diffraction analysis (XRD) are shown in **Table 1**. The results show that the *TOC* of the Dongyuemiao Member varies within a large range from 0.58 to 1.96%, with an average of 1.52%. The variation range of the Da'anzhai Member is relatively small, from 0.70 to 1.33%, with an average of 1.00%. Compared with the *TOC* contents of the Lower Silurian or Lower Cambrian marine shale in the Sichuan Basin, the *TOC* content is lower, mainly because the marine shale organic matter is derived from the deep sea or semideep sea, where abundant microorganisms are deposited in the reducing environment (Liang et al., 2014; Li et al., 2015; Jin et al., 2016; Nie et al., 2016; Sun et al., 2016; Nie et al., 2017a; Jin et al., 2018; Zhao et al., 2019). However, the major source of organic matter in continental shale is higher plants, which are more likely to be affected by water depth, material sources, and deposition rates than marine shale (Wei et al., 2014).

The lower limit of R_o in the shale gas prospect area is 0.65% and in the favorable area is 1.0% of continental Basin in China in the simulation experiment of the hydrocarbon generation of low matured shale. The R_o of the Dongyuemiao Member in the Fuling area is between 0.96 and 1.19% and that of the Da'anzhai Member in the Yuanba block is between 1.31 and 1.44%.

Appropriate evolution and high organic matter content are the vital foundations for hydrocarbon generation and pore formation (Jiang et al., 2019; Zhang et al., 2020b). In general, although the *TOC* and R_o of continental shale are lower than those of marine shale, the thickness of continental shale reservoirs is large, and the organic matter is in the mature stage. Therefore, the continental organic matter has the ability to generate gas and pores.

Continental Shale Reservoir Mineral Composition

The main components of the shale are clay minerals, siliceous minerals (quartz and feldspar), and other authigenic minerals (pyrite and carbonate). The analyzed XRD results in **Table 1**
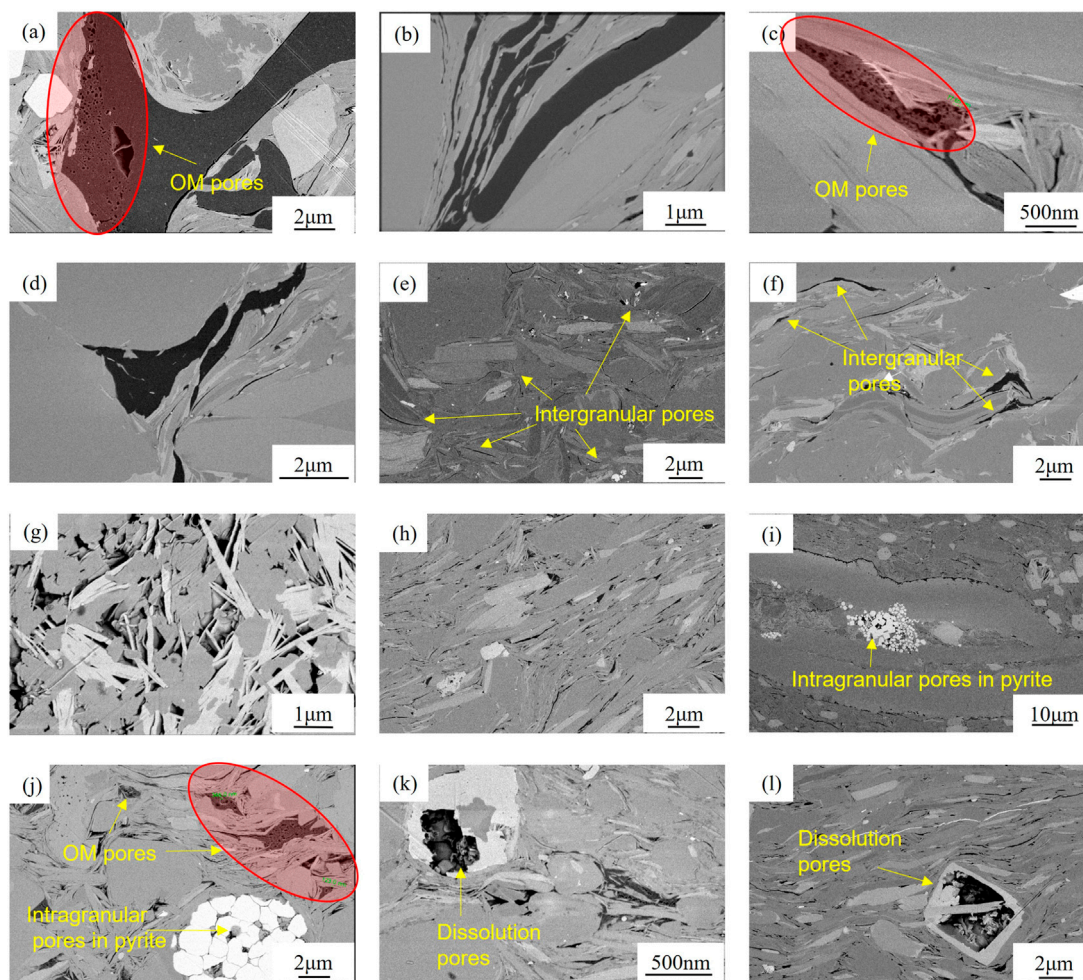
FIGURE 2 | Pores of the continental shale reservoir in northeastern Sichuan Basin. **(A)** Da'anzhai Member from YL-4 Well, 3748.23 m, organic matter pores; **(B)** Da'anzhai Member from YL-4 Well, 3760.75 m, dense structure of organic matter without organic matter pores; **(C)** Dongyuemiao Member from FY-1 Well, 2736.30 m, organic matter pores; **(D)** Dongyuemiao Member from XL-101 Well, 2294.33 m, dense structure of organic matter without organic matter pores; **(E)** Da'anzhai Member from YL-4 Well, 4051.81 m, interparticle pores; **(F)** Dongyuemiao Member from XL-101 Well, 2294.33 m, a small amount of bitumen filled in intergranular pores and poor development of pores; **(G)** Da'anzhai Member from YL-4 Well, 3790.14 m, micropores between clay minerals; **(H)** Dongyuemiao Member from XL-101 Well, 2275.55 m, micropores between clay minerals which are filled with bitumen; **(I)** Da'anzhai Member from YL-4 Well, 3748.23 m, intragranular pores in pyrite; **(J)** Dongyuemiao Member from FY-1 Well, 2708.41 m, intragranular pores in pyrite and organic matter pores in bitumen; **(K)** Da'anzhai Member from YL-4 Well, 3790.14 m, dissolution pores in the ankerite; **(L)** Dongyuemiao Member from XL-101 Well, 2269.69 m, dissolution pores in the ankerite.

show that the content of clay minerals ranges from 43.1 to 63.9%, with an average of 58.7%, and the content of quartz is between 20.1 and 42.7%, with an average of 26.5% in the Dongyuemiao Member in the Fuling area. The clay mineral content ranges from 38.8 to 65.3% with a 51.8% average, the quartz content is between 26.4 and 50.3%, and the average is 33.6% in the Da'anzhai Member in the Yuanba area. The continental shale reservoir mainly comprises clay minerals, followed by quartz, and carbonate minerals are locally developed, which account for 20% of the total mineral content.

Pore Types of Continental Shale Reservoirs

The pore types of shale reservoirs are classified by various methods, mainly according to size, origin, and morphology (Slatt and O'Brien, 2011; Zou et al., 2011; Loucks et al., 2012;

Zou et al., 2013). According to the scanning electron microscopy observations conducted after the argon-ion polishing techniques, the pores of continental shale reservoirs can be divided into two categories: shale pores and interlayer pores. The former mainly includes organic matter pores, mineral matrix pores, and microcracks. The latter is formed by tectonics and dissolution.

Organic Matter Pores

The organic matter pores are formed in the processes of the pyrolysis and hydrocarbon generation of the organic matter in shale. It is generally believed that the organic matter pores are the main pore type and are one of the key factors in the accumulation of shale gas (Loucks et al., 2009; Guo et al., 2014; Romero-Sarmiento et al., 2014). The organic matter of continental shale mainly consists of vitrinite and fusinite, followed by solid

bitumen. The results of the scanning electron microscopy conducted after the argon-ion polishing techniques show that different macerals generate different pores. The vitrinite formed by the humification and gelation function of the wood fiber tissue from higher plants and the fusinite formed by the carbonization function of the wood fiber tissue from higher plants do not develop organic matter pores, while the hydrogen-rich vitrinite influenced by microorganisms and solid bitumen develop different levels of organic matter pores (**Figures 2A–D**). The diameters of the organic matter pores are mainly distributed in the range of 2 nm–2 μm, with a large proportion of mesopores, which contributes more to the specific surface area and pore volume of shale, so it plays a positive role in the accumulation of shale gas.

Mineral Matrix Pores

By conducting scanning electron microscopy after argon-ion polishing techniques, it can be seen that the mineral matrix pores of the Ziliujing Formation in the study area consist of four types: interparticle pores, pores between clay minerals, pores between pyrite, and secondary dissolution pores.

The interparticle pores are one of the main pore types observed in the study area, which are residual primary pores formed by quartz, feldspar, carbonate minerals, and clay mineral (such as illite and chlorite) particle arrangement accumulation and diagenetic compaction between the grains (Yang Chao et al., 2014; Cao et al., 2015; Guan et al., 2016; Li et al., 2019). By observation and analysis, the mineral matrix pores are mainly pores that are developed between minerals and between mineral particles and clay minerals (**Figures 2E,F**). Most of them are triangular, polygonal, oblong, and irregular. The pore size range is large. In addition, nanopores and micropores are developed and mainly formed by the contact of brittle particles and plastic

particles. In the early stage, the intergranular pores with large pore sizes were mostly filled with bitumen, and the intergranular pores with relatively small pore sizes were partly preserved due to the support structure formed by the chaotic accumulation between clay minerals and rigid grains or clay minerals.

The pores between clay minerals are mainly micropores between illite. When the pore water of shale is relatively alkaline and rich in potassium ions, as the burial depth increases, montmorillonite will transform into illite, and the volume will decrease, resulting in microcracks (or micropores) (Yang Chao et al., 2014; Cao et al., 2015; Guan et al., 2016; Li et al., 2019). Mesopores between clay minerals are extensively developed in the Ziliujing Formation in the study area (**Figures 2G,H**), mainly in layers of illites and illites and micas. The linear pores have different lengths and widths and can appear as slits, triangles, or polygons, controlled by the organic carbon content and the development of pores, and these pores have different occupied spaces of bitumen, including whole-filling, half-filling, part-filling, and no filling. These pores are formed by early clay mineral pores decreasing rapidly under strong compaction with the continuous increase in burial depth and are the most common pores in the study area.

The pores between pyrite framboids are intergranular pores that are formed by mineral crystallization under a stable environment and appropriate medium conditions. Most of the pyrites in continental reservoirs appear as single crystals, and only a few are "strawberry" pyrites. These pores are relatively few (**Figures 2G,I**).

The secondary dissolution pores are secondary pores formed by the dissolution of minerals that can be dissolved easily, such as feldspar and carbonate, under the acidic water produced by the decarboxylation of groundwater or organic matter. Such pores can be divided into intraparticle and interparticle dissolution
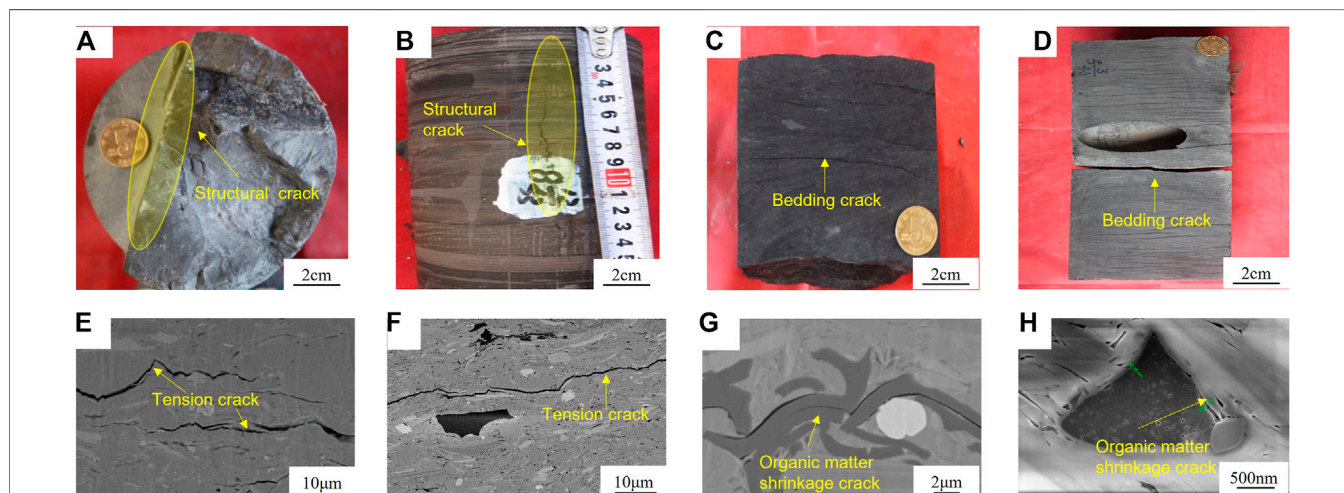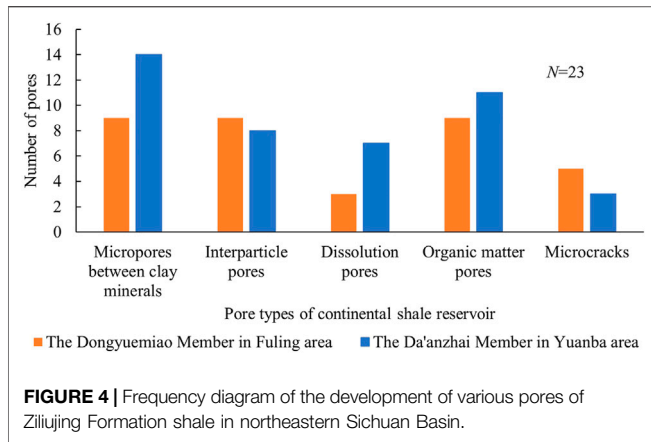

FIGURE 3 | Microcracks of the continental shale reservoir in northeastern Sichuan Basin. **(A)** Da'anzhai Member from YL-4 Well, 4004.25–4004.43 m, structural crack without filling; **(B)** Dongyuemiao Member from FY-1 Well, 2707.2–2707.4 m, structural crack; **(C)** Da'anzhai Member from YL-4 Well, 4053.12—4053.22 m, bedding crack; **(D)** Dongyuemiao Member from XL-101 Well, 2268.97–2269.12 m, bedding crack; **(E)** Da'anzhai Member from YL-4 Well, 3789.34 m, microscopic tension crack; **(F)** Dongyuemiao Member from XL-101 Well, 2275.55 m, microscopic tension crack; **(G)** Da'anzhai Member from YL-4 Well, 3789.34 m, organic matter shrinkage crack; **(H)** Dongyuemiao Member from XL-101 Well, 2269.69 m, organic matter shrinkage crack.

FIGURE 4 | Frequency diagram of the development of various pores of Ziliujing Formation shale in northeastern Sichuan Basin.
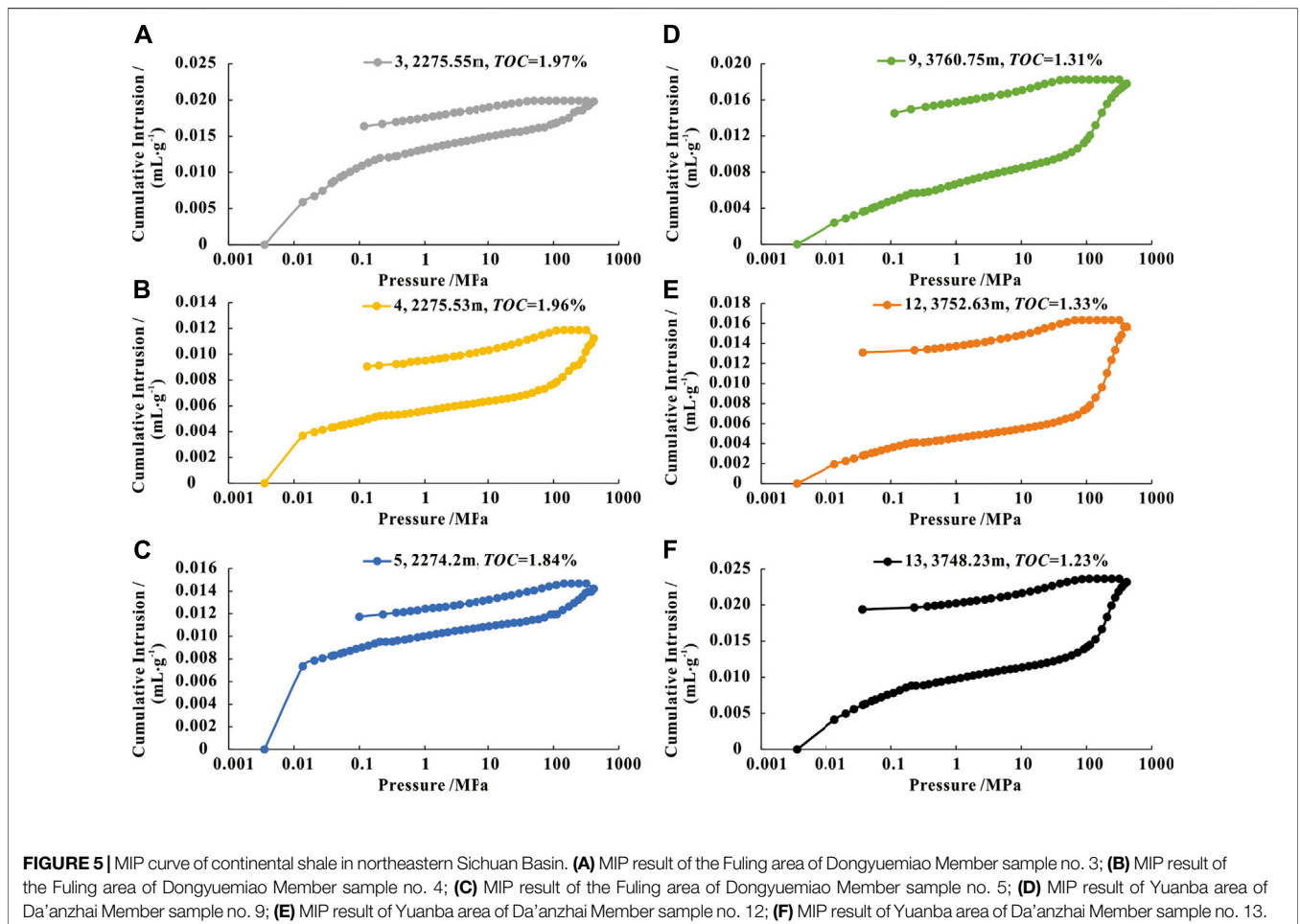
role in the exploitation of shale gas. According to their sizes, the cracks are divided into two types: macroscopic cracks and microcracks. Macroscopic cracks can be observed through the cores, which mainly include structural cracks and bedding cracks (**Figures 3A–D**). The cracks observed by scanning electron microscopy are collectively called microcracks, which mainly include microscopic tension cracks and organic matter shrinkage cracks (**Figures 3E–H**).
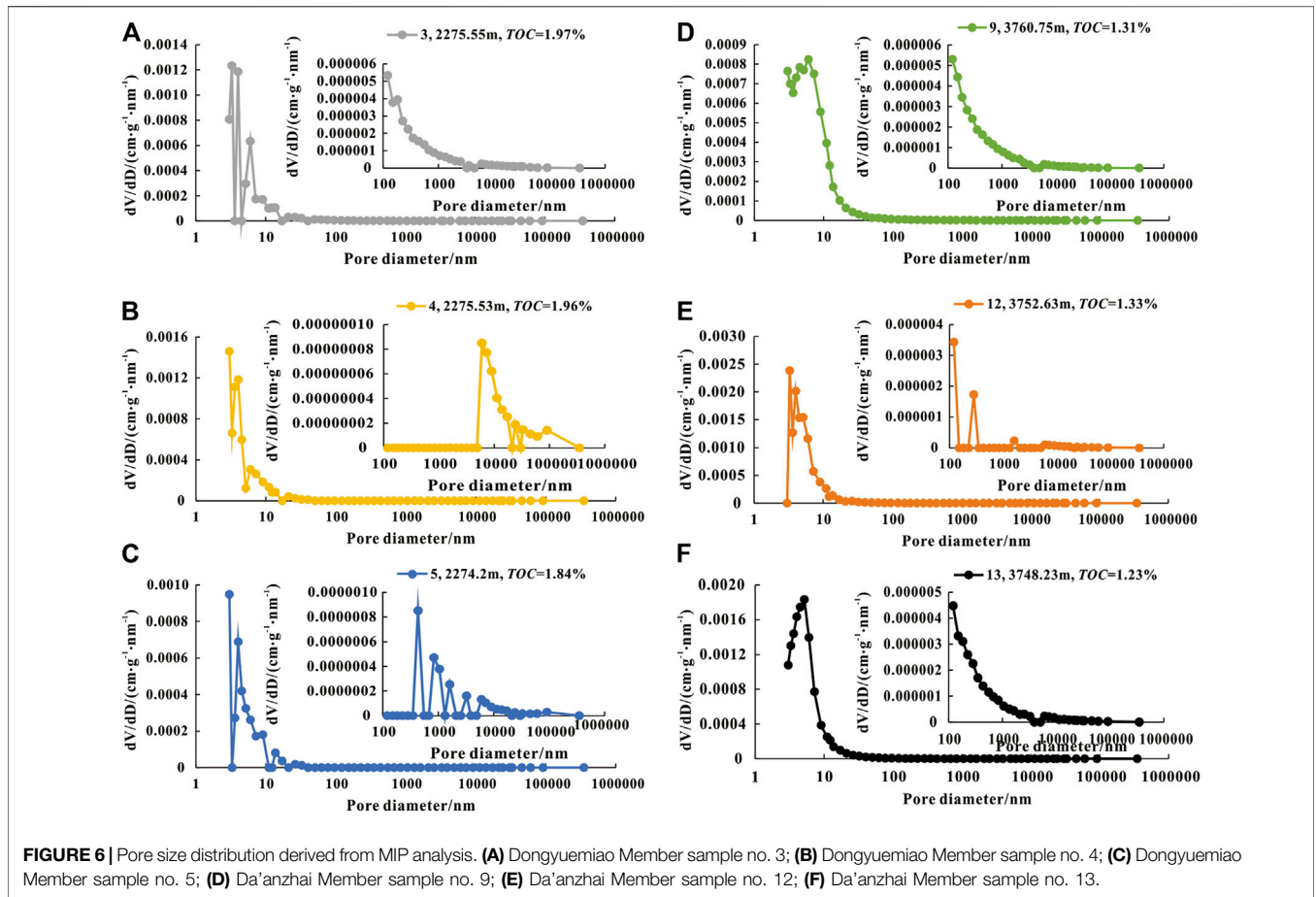
According to the statistics of the scanning electron microscopy and core observations, as can be seen from **Figure 4**, the pores of the continental shale reservoirs in the northeastern Sichuan Basin are dominated by mineral matrix pores, followed by organic matter pores, and microcracks are developed locally.

pores (**Figures 2K,L**). The sizes of the former are smaller, mainly 0.05–4 μm. The sizes of the latter are larger, mainly 1–4 μm.

Microcracks

The crack system developed in the shale reservoir is not only conducive to the accumulation of free gas but also the main channel for the seepage migration of shale gas, which plays a key

Pore Characteristics of Shale Based on Various Experiments

Characteristics of the Pore Size Distribution of Continental Shale Based on Mercury Injection Experiments

The developmental characteristics of larger shale pores can be indicated by mercury intrusion curves, and **Figure 5** shows the difference between the two regions. In the case of the Da'anzhai

FIGURE 5 | MIP curve of continental shale in northeastern Sichuan Basin. **(A)** MIP result of the Fuling area of Dongyuemiao Member sample no. 3; **(B)** MIP result of the Fuling area of Dongyuemiao Member sample no. 4; **(C)** MIP result of the Fuling area of Dongyuemiao Member sample no. 5; **(D)** MIP result of Yuanba area of Da'anzhai Member sample no. 9; **(E)** MIP result of Yuanba area of Da'anzhai Member sample no. 12; **(F)** MIP result of Yuanba area of Da'anzhai Member sample no. 13.

FIGURE 6 | Pore size distribution derived from MIP analysis. **(A)** Dongyuemiao Member sample no. 3; **(B)** Dongyuemiao Member sample no. 4; **(C)** Dongyuemiao Member sample no. 5; **(D)** Da'anzhai Member sample no. 9; **(E)** Da'anzhai Member sample no. 12; **(F)** Da'anzhai Member sample no. 13.

Member of the Yuanba area, the low-pressure part ($p < 0.2$ MPa) mainly develops pores larger than 6 µm, and the amount of mercury increases with increasing pressure. When the pressure reaches 0.2 MPa, the increase in mercury inflow slows; when the pressure is between 0.2 and 0.3 MPa, the amount of mercury entering is small, indicating that this pressure range corresponds to less pore development. At pressures greater than 0.3 MPa, the amount of mercury ingress begins to increase with increasing pressure. The difference in the volume of mercury in and out indicates that there is a low mercury withdrawal rate, poor connectivity, and strong heterogeneity.
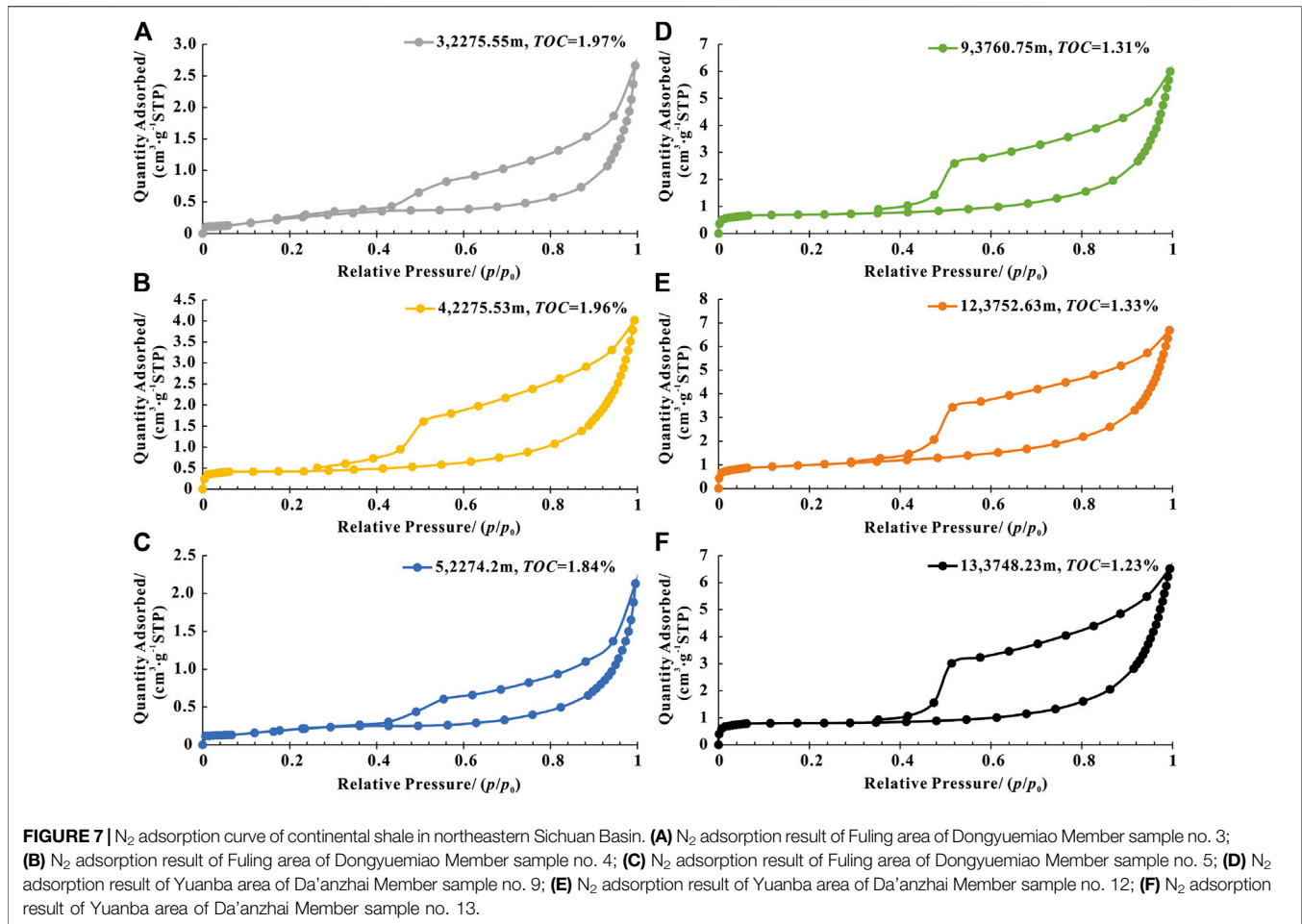
The front member of the curve in Dongyuemiao in the Fuling area is similar to that in the Yuanba area. When the pressure reaches 100 MPa, a small amount of mercury is still shown on the curve in terms of the Fuling area. The difference in the volumes of mercury in and out is relatively small, indicating a higher mercury rejection rate and better connectivity. In general, the continental shale in northeastern Sichuan develops macropores, and the Dongyuemiao Member of the Fuling area has more open pores with better connectivity than the Da'anzhai Member of the Yuanba area.

The pore size distribution curves of the shale samples are shown in **Figure 6**. There are multiple peaks on the curves, and most of the peaks exist between 3 and 30 nm. The second peak of the sample from the Fuling area appeared after 1 µm, while the

peak of the sample from the Yuanba area is continuous. The pore volume of the shale in the Ziliujing Formation mainly comprises mesopores in the range of 3–30 nm, followed by macropores. Compared to those of the Dongyuemiao Member, the macropores in the Da'anzhai Member have better development, a more uniform pore size distribution, and a greater contribution to the pore volume.

Pore Distribution Characteristics of Continental Shale Based on N₂ Adsorption Experiments

The small shale pore characteristics can be analyzed by N_2 adsorption experiments through adsorption–desorption curves. **Figure 7** shows that the nitrogen adsorption curve of the shale sample is generally the opposite "S" type. When the relative pressure is low ($0 < p/p_0 < 0.3$), the adsorption amount rises slowly, and the adsorption isotherm slightly bulges upward. At this time, for the adsorption of the monolayer to the multimolecular layer, the inflection point of the isotherm adsorption line is usually the turning point. At medium–high relative pressure ($0.3 < p/p_0 < 0.8$), the adsorption layer is a multilayered molecule, and the adsorption amount increases slowly. At high relative pressure ($0.8 < p/p_0 < 1$), the adsorption amount increases sharply, and the curve shape shows a downward concave trend. Until the relative pressure is close to 1, there is no saturated adsorption phenomenon,

FIGURE 7 | N₂ adsorption curve of continental shale in northeastern Sichuan Basin. **(A)** N₂ adsorption result of Fuling area of Dongyuemiao Member sample no. 3; **(B)** N₂ adsorption result of Fuling area of Dongyuemiao Member sample no. 4; **(C)** N₂ adsorption result of Fuling area of Dongyuemiao Member sample no. 5; **(D)** N₂ adsorption result of Yuanba area of Da'anzhai Member sample no. 9; **(E)** N₂ adsorption result of Yuanba area of Da'anzhai Member sample no. 12; **(F)** N₂ adsorption result of Yuanba area of Da'anzhai Member sample no. 13.

indicating that the capillary condensation of absorbed N_2 occurs on the shale surface due to the presence of the mesopores and macropores in the shale of Ziliujing.
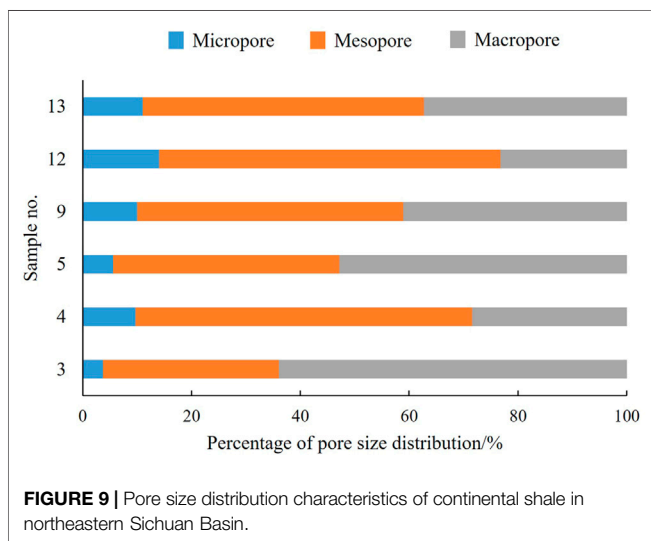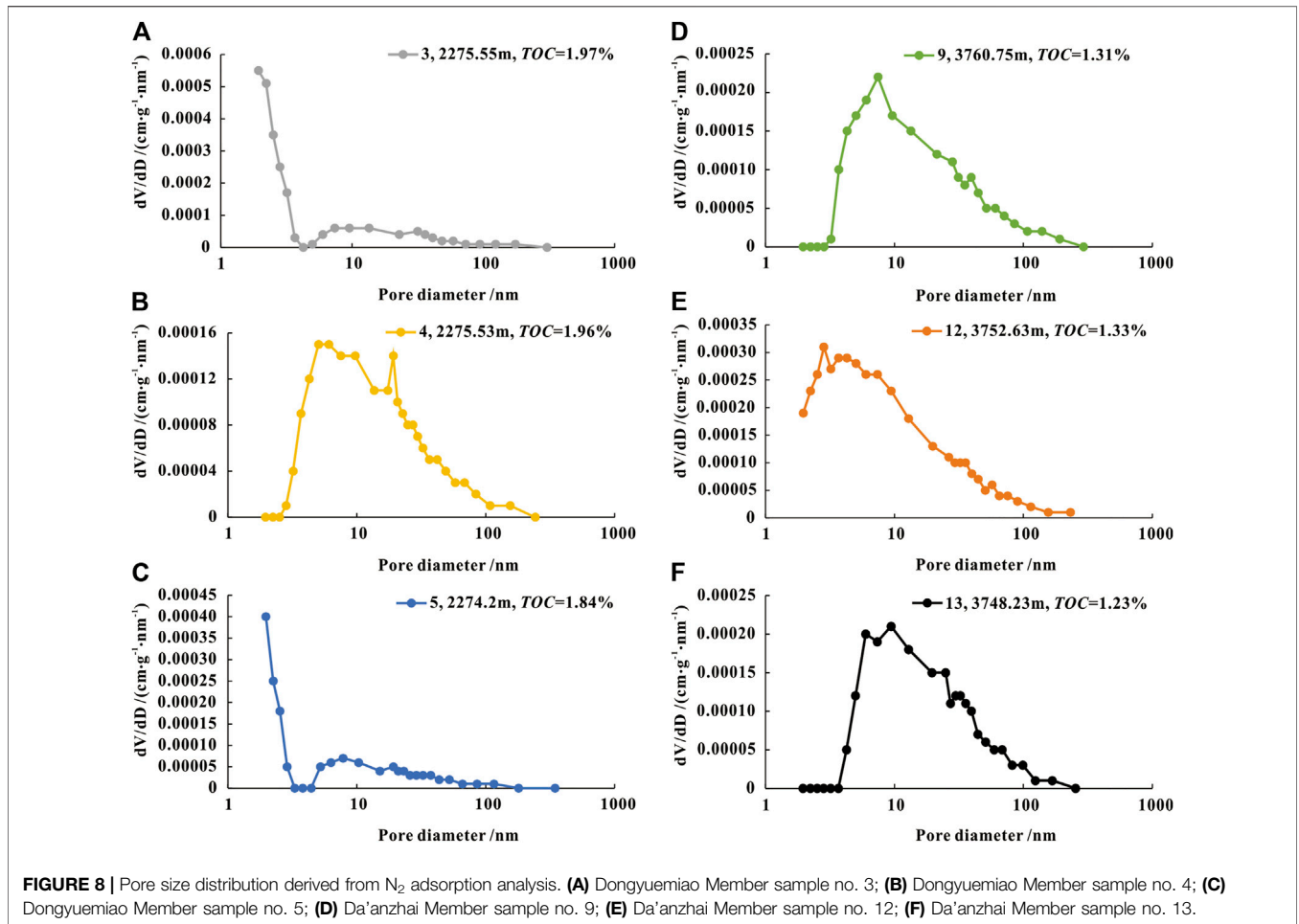
When the relative pressure $p/p_0 > 0.3$, the adsorption and desorption isotherms are separated to form a hysteresis loop. The width of the loop of the Da'anzhai Member sample is significantly wider than that of the Dongyuemiao sample, which indicates that the pore size distribution in Da'anzhai is more uniform and wider. The hysteresis loop of shale is divided into four types by the International Union of Pure and Applied Chemistry (IUPAC; Sing et al., 1985). The hysteresis loop of the Ziliujing sample is close to H3 and H4 in terms of morphology. The shale sample mainly develops parallel plate-like slit-type pores and contains a small amount of ink bottle–shaped pores (IUPAC; Sing et al., 1985), which have good connectivity and are favorable for the seepage and development of shale gas.

Figure 8 shows the pore size distribution curves of the shale samples obtained from the N_2 adsorption experiments. The change rates of the pore volume are mainly in the range of 3–30 nm and decrease with increasing pore size, indicating that the pore volume mainly comprises pores between 3 and 30 nm, which is consistent with the conclusion, obtained using the mercury porosimetric method.

Characterization of all Pore Sizes of Continental Shale

The full pore size distribution of shale can be calculated from the results of the N_2 adsorption and high-pressure mercury intrusion experiments (**Figure 9**). The pore volume of the sample from Dongyuemiao in the Fuling area is between 0.00412 and 0.00727 cm^3/g, with an average of 0.00577 cm^3/g, and the specific surface area is between 0.772 and 3.250 m^2/g, with an average of 1.496 m^2/g. Most of the pores are mesopores, ranging from 32.4 to 62.8%, with an average of 50.517%, mainly between 10 and 50 nm. This was followed by macropores, accounting for 13.3–63.9%, with an average of 38.7%, mainly between 1 and 5 μm. Microporous development is very small, accounting for only 3.7–29.3%. The pore volume of the sample from the Da'anzhai Member of the Yuanba area is between 0.0086 and 10.0136 cm^3/g, with an average of 0.0113 cm^3/g, and the specific surface area is between 2.206 and 6.918 m^2/g, with an average of 3.987 m^2/g. Most of the pores are mesopores, accounting for 48.9–62.7%, with an average of 56.3%, mainly between 10 and 50 nm. This was followed by macropores, accounting for 14.4–43.7%, with an average of 28.9%, mainly between 1 and 5 μm. Micropores account for only 10.0–25.6%.

It is suggested that most of the continental shale pores in the study area are mesopores, followed by macropores and micropores, mainly between 10 and 50 nm, followed by 1–5 μm. The mesopores

FIGURE 8 | Pore size distribution derived from N₂ adsorption analysis. **(A)** Dongyuemiao Member sample no. 3; **(B)** Dongyuemiao Member sample no. 4; **(C)** Dongyuemiao Member sample no. 5; **(D)** Da'anzhai Member sample no. 9; **(E)** Da'anzhai Member sample no. 12; **(F)** Da'anzhai Member sample no. 13.

FIGURE 9 | Pore size distribution characteristics of continental shale in northeastern Sichuan Basin.

and macropores may form from clay minerals, and the pore volume is increased due to secondary dissolution pores and cracks, which are related to high calcite content. The micropores are blocked by the soluble organic matter, which is formed by hydrocarbon generation. Such a pore size distribution type is more beneficial to the enrichment of free gas.

DISCUSSION

Effects of *TOC* Content and Mineral Composition on Pore Structure

By analyzing the correlation of pore structural parameters (pore volume and specific surface area) and $T`OC$ content, the brittle and clay mineral contents of the continental shale reservoirs in the study area (**Figure 10**) indicate that the pore volume and specific surface area are negatively correlated or irrelevant to the TOC content (**Figures 10A,B**). This is because the organic matter is mostly vitrinite and inertinite, organic matter pores are not developed (**Figures 2B,D**), and the soluble organic matter that is formed during organic matter generation occupies the pores and adsorption sites, causing a decrease in the pore quantity in low-maturity shale (Li et al., 2017; Cao et al., 2018).

The pore volume is positively correlated with the clay mineral content and negatively correlated with the quartz content (**Figures 10B,C**), confirming that clay mineral pores are the

FIGURE 10 | Relationship between pore structure parameters and *TOC* and mineral content of Ziliujing Formation in northeastern Sichuan Basin. **(A)** Relationship between pore volume and *TOC*; **(B)** Relationship between pore volume and clay compositions; **(C)** Relationship between pore volume and quartz; **(D)** Relationship between surface area and *TOC*; **(E)** Relationship between surface area and clay compositions; **(F)** Relationship between surface area and quartz.

main pore type of continental shale. The correlations are not so strong, which illustrates that the pore volume is comprehensively controlled by multiple factors.

The specific surface area is not related to the mineral content and quartz content of the sample from the Da'anzhai Member and negatively correlated with the clay minerals and positively correlated with the quartz content of the sample from the Dongyuemiao Member (**Figures 10E,F**). It is shown that the pore size and range of the pore size between clay minerals are large, and the small pores are mainly constituted by the dissolved pores and intergranular pores formed by rigid minerals and clay minerals, which mainly contribute to the specific surface area.

Reservoir Capacities of the Continental Shale Reservoirs in the Northeastern Sichuan Basin

Natural gas can be stored in three ways, adsorbed, free, and dissolved gas, in two main storage sites with adsorbed reservoir space and free reservoir space (Ross et al., 2006; Hickey and Henk, 2007). The diversity in the formation of free shale gas reservoir space (comprising mesopores to macropores) and adsorbed shale gas reservoir space (comprising micropores to mesopores) is determined by the differences in the facies association, total organic carbon (*TOC*), maturity of organic matter (R_o), organic matter types, and overpressure in the reservoir (Schettler and Parmoly, 1990; Lu et al., 1995; Pollastro, 2002;

Jarvie et al., 2007; Chalmers and Bustin, 2008; Ross and Bustin, 2008; Zhang et al., 2012).

A two-factor method is used to evaluate reservoir capacity based on research on the pore structure and uses the normalized ratio of pore volume to surface area as an index of gas storage capacity in distinguishing the adsorbed reservoir space and free reservoir space. According to the practical production record, the

FIGURE 11 | Reservoir capacity of continental shale reservoirs in the northeastern Sichuan Basin (JY1 well data by the Guo et al., 2014; FYX well data by the Sinopec).
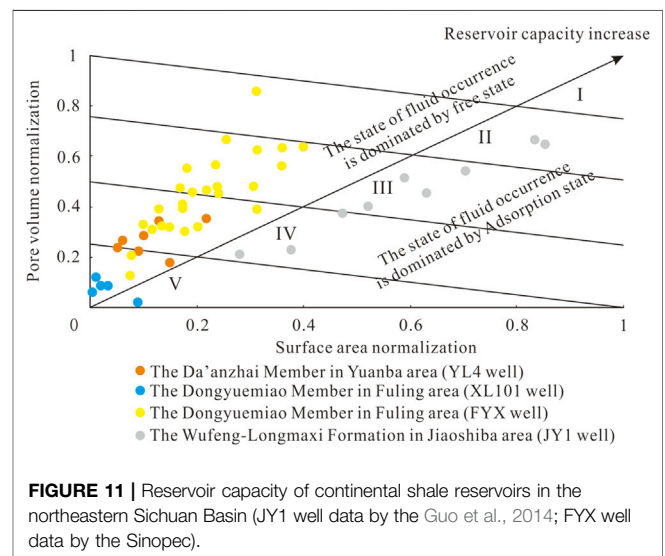
ratio of free gas to adsorbed gas is usually 3/1, which is more suitable for mining, and the S/V is identified with 0.25, 0.5, 0.75, and 1 as the criteria for dividing the levels of reservoirs (Zhao et al., 2016; Zhao et al., 2017; Hu et al., 2018). This method uses data from forming well-studied shale gas reservoirs as standards and can be efficient and straightforward in comparing the storage capacities of different wells and study areas.

In this study, we summarize our samples, that is, the samples from the continental shale gas FYX well in the Fuling area and the JY1 well in the shale gas main productive location in China in the Jiaoshiba area. The relationship between the normalized pore volume and surface area data is shown in **Figure 11**. **Figure 11** shows the storage capacity of the XL101 well, the YL4 well, and the FYX well levels V, IV, and III–IV, respectively. The storage capacity of JY1 decreases from bottom to top and levels II–III. Compared with marine shale, the reservoir morphology of continental shale is freer. Marine shale gas storage comprises organic pores and type I kerogen, with an average *TOC* of 2.65% and an organic matter (R_o) maturity of approximately 2.6%, which makes it possible to form many organic pores with pore diameters <24 nm and fewer macropores. In contrast, continental shale gas storage has type II–III kerogen, with an average *TOC* of 1.24% and an organic matter (R_o) maturity of approximately 1.2%. The pores originate from clay minerals with less organic matter; only hydrogen-rich vitrinite and solid asphalt develop organic pores, which are macropores. The continental shale has a pore diameter of 10–50 nm with predominant macropores and fewer micropores.

According to the analysis in the field, the average gas content of the JY1 well is 2.96 m^3/t, that of the YL4 well is 1.374 m^3/t, and that of the XL101 well is 1.183 m^3/t, which is highly consistent with the evaluation of the reservoir storage capacities.

CONCLUSION

1) The pores of the continental shale reservoirs in the northeastern Sichuan Basin are dominated by mineral matrix pores, followed by organic matter pores, and microcracks are developed locally.
2) The characteristics of the pore structures in the two layers of continental shale were measured using high-pressure mercury injection and nitrogen adsorption methods. The results show that the pores consist of predominant mesopores (10–50 mm) followed by some macropores because the high content of clay minerals in the continental shale reservoirs provides mostly mesopores to macropores. In addition, a high concentration of carbonate forms corrosion apertures and raises the volume of pores. With hydrocarbon generation, soluble organic matter jams micropores. The characteristics of the pore structure result in an abundance of free gas.
3) The ratio of pore volume to surface area shows a negative correlation or is uncorrelated with the total organic carbon (*TOC*) content. The organic matter in the continental shale is usually vitrinite and fusinite that evolved from the wooden fibrous histiocytoma in higher plants, which do not develop organic pores. Clarovitrinite and solid bitumen develop organic

pores with various pore diameters. The positive correlation of the pore volume with the clay mineral concentration indicates that the main type of pore structure in the continental shale reservoirs is pores between clay minerals, while the lack of correlations shows that a number of factors determine pore volume. The ratio of pore volume to surface area has a positive correlation with the quartz content in the sample from the Dongyuemiao member in the Fuling area and indicates that micropores originate from dissolution pores and intergranular pores between rigid minerals and clay minerals.

4) We evaluated the reservoir capacities of the continental shale reservoirs in the northeastern Sichuan Basin by using a method of the normalized ratio of pore volume to surface area two-factor method with the Lower Silurian marine shale reservoir from the Jiaoshiba area in the Sichuan Basin as a benchmark. The continental shale reservoirs mainly show free-state accumulation from level II to level IV. This reservoir mostly comprises clay mineral pores and consists of mesopores to macropores, which are beneficial for the accumulation of free gas.

DATA AVAILABILITY STATEMENT

The original contributions presented in the study are included in the article/Supplementary Materials, further inquiries can be directed to the corresponding author.

AUTHOR CONTRIBUTIONS

TJ: conceptualization, data curation, formal analysis, methodology, resources, software, supervision, investigation, writing—original draft, and review and editing. ZJ: funding, supervision, resources, and methodology. GL: funding, supervision, investigation, resources, and methodology. ZH: funding, supervision, investigation, and resources. XC: resources, methodology, and formal analysis. ZL: supervision, methodology, data curation, resources, and writing–review and editing. GW: supervision, resources, methodology, formal analysis, investigation, manuscript writing and review and editing.

REFERENCES

Cao, T., Deng, M., Liu, H., Song, Z., Cao, Q., and Huang, Y. (2018). Influences of Soluble Organic Matter on Reservoir Properties of Shale. *Lithologic Reservoirs* 30 (03), 43–51. (in Chinese with English abstract).

Cao, T., Song, Z., Wang, S., Cao, X., Li, Y., and Xia, J. (2015). Characterizing the Pore Structure in the Silurian and Permian Shales of the Sichuan Basin, China. *Mar. Pet. Geology*. 61, 140–150. doi:10.1016/j.marpetgeo.2014.12.007

Chalmers, G. R., Bustin, R. M., and Power, I. M. (2012). Characterization of Gas Shale Pore Systems by Porosimetry, Pycnometry, Surface Area, and Field Emission Scanning Electron Microscopy/transmission Electron Microscopy Image Analyses: Examples from the Barnett, Woodford, Haynesville, Marcellus, and Doig Units. *Bulletin* 96 (6), 1099–1119. doi:10.1306/10171111052

Chalmers, G. R. L., and Bustin, R. M. (2008). Lower Cretaceous Gas Shales in Northeastern British Columbia, Part I: Geological Controls on Methane Sorption Capacity. *Bull. Can. Pet. Geology*. 56 (1), 1–21. doi:10.2113/gscpgbull.56.1.1

Chen, L., Jiang, Z., Liu, K., Wang, P., Gao, F., and Hu, T. (2017). Application of Low-Pressure Gas Adsorption to Nanopore Structure Characterisation of Organic-Rich Lower Cambrian Shale in the Upper Yangtze Platform, South China. *Aust. J. Earth Sci.* 64 (5), 653–665. doi:10.1080/08120099.2017.1334705

Chen, L., Jiang, Z., Liu, K., Wang, P., Ji, W., Gao, F., et al. (2016). Effect of Lithofacies on Gas Storage Capacity of marine and continental Shales in the Sichuan Basin, China. *J. Nat. Gas Sci. Eng.* 36, 773–785. doi:10.1016/j.jngse.2016.11.024

Chen, S., Zhu, Y., Wang, H., Liu, H., Wei, W., and Fang, J. (2011). Shale Gas Reservoir Characterisation: A Typical Case in the Southern Sichuan Basin of China. *Energy* 36, 6609–6616. doi:10.1016/j.energy.2011.09.001

Curtis, J,B. (2002). Fractured Shale-Gas Systems. *AAPG Bulletion* 86 (11), 1921–1938. doi:10.1306/61eeddbe-173e-11d7-8645000102c1865d

Curtis, M. E., Cardott, B. J., Sondergeld, C. H., and Rai, C. S. (2012). Development of Organic Porosity in the Woodford Shale with Increasing thermal Maturity. *Int. J. Coal Geology*. 103 (3), 26–31. doi:10.1016/j.coal.2012.08.004

Deng, K. (1992). Formation and Evolution of Sichuan basin and Domains for Oil and Gas Exploration. *Nat. Gas Industry* 12 (5), 7–12+6. (in Chinese with English abstract).

Dong, D., Wang, Y., Li, X., Zou, C., Guan, Q., Zhang, C., et al. (2016a). Breakthrough and prospect of Shale Gas Exploration and Development in China. *Nat. Gas Industry* 36 (01), 19–32. (in Chinese with English abstract). doi:10.1016/j.ngib.2016.02.002

Dong, D., Zou, C., Dai, J., Huang, S., Zheng, J., Gong, J., et al. (2016b). Suggestions on the Development Strategy of Shale Gas in Cina. *Nat. Gas Geosci.* 27 (03), 397–406. (in Chinese with English abstract).

Guan, Q., Dong, D., Wang, S., Huang, J., Wang, Y., and Zhang, C. (2016). Analyses on Differences of Microstructure between marine and Lacustrine Facies Shale Reservoirs. *Nat. Gas Geosci.* 27 (03), 524–531. (in Chinese with English abstract).

Guo, S., Mao, W., and Ma, X. (2017). Thermal Simulation experiment Study of the Hydrocarbon Generation Characteristics of Low Maturity Shale. *Earth Sci. Front.* 24 (6), 365–369. (in Chinese with English abstract).

Guo, X., Hu, D., Wei, Z., Li, Y., and Wei, X. (2016). Discovery and Exploration of Fuling Shale Gas Field. *China Pet. Exploration* 21 (3), 24–37. (in Chinese with English abstract).

Guo, X., Li, Y., Liu, R., and Wang, Q. (2014). Characteristics and Controlling Factors of Micro-pore Structures of Longmaxi Shale Play in the Jiaoshiba Area, Sichuan Basin. *Nat. Gas Industry* 34 (06), 9–16. (in Chinese with English abstract).

Han, C., Jiang, Z., Han, M., Wu, M., and Lin, W. (2016). The Lithofacies and Reservoir Characteristics of the Upper Ordovician and Lower Silurian Black Shale in the Southern Sichuan Basin and its Periphery, China. *Mar. Pet. Geology*. 75, 181–191. doi:10.1016/j.marpetgeo.2016.04.014

Hao, F., Zou, H., and Lu, Y. (2013). Mechanisms of Shale Gas Storage: Implications for Shale Gas Exploration in China. *Bulletin* 97 (8), 1325–1346. doi:10.1306/02141312091

Hickey, J. J., and Henk, B. (2007). Lithofacies Summary of the Mississippian Barnett Shale, Mitchell 2 T.P. Sims Well, Wise County, Texas. *Bulletin* 91 (4), 437–443. doi:10.1306/12040606053

Hu, H., Hao, F., Guo, X., Dai, F., Lu, Y., and Ma, Y. (2018). Investigation of Methane Sorption of Overmature Wufeng-Longmaxi Shale in the Jiaoshiba Area, Eastern Sichuan Basin, China. *Mar. Pet. Geology*. 91, 251–261. doi:10.1016/j.marpetgeo.2018.01.008

Jarvie, D. M., Hill, R. J., Ruble, T. E., and Pollastro, R. M. (2007). Unconventional Shale-Gas Systems: The Mississippian Barnett Shale of north-central Texas as One Model for Thermogenic Shale-Gas Assessment. *Bulletin* 91 (4), 475–499. doi:10.1306/12190606068

Ji, W., Song, Y., Jiang, Z., Meng, M., Liu, Q., Chen, L., et al. (2016). Fractal Characteristics of Nano-Pores in the Lower Silurian Longmaxi Shales from the Upper Yangtze Platform, south China. *Mar. Pet. Geology*. 78, 88–98. doi:10.1016/j.marpetgeo.2016.08.023

Ji, W., Song, Y., Jiang, Z., Wang, X., Bai, Y., and Xing, J. (2014). Geological Controls and Estimation Algorithms of Lacustrine Shale Gas Adsorption Capacity: a Case Study of the Triassic Strata in the Southeastern Ordos Basin, China. *Int. J. Coal Geology*. 134-135 (135), 61–73. doi:10.1016/j.coal.2014.09.005

Jiang, T., Jin, Z., Liu, G., Liu, Q., Gao, B., Liu, Z., et al. (2019). Source Analysis of Siliceous Minerals and Uranium in Early Cambrian Shales, South China: Significance for Shale Gas Exploration. *Mar. Pet. Geology*. 102, 101–108. doi:10.1016/j.marpetgeo.2018.11.002

Jin, Z., Hu, Z., Gao, B., and Zhao, J. (2016). Controlling Factors on the Enrichment and High Productivity of Shale Gas in the Wufeng-Longmaxi Formations, southeastern Sichuan Basin. *Earth Sci. Front.* 23 (1), 1–10. (in Chinese with English abstract).

Jin, Z., Nie, H., Liu, Q., Zhao, J., and Jiang, T. (2018). Source and Seal Coupling Mechanism for Shale Gas Enrichment in Upper Ordovician Wufeng Formation - Lower Silurian Longmaxi Formation in Sichuan Basin and its Periphery. *Mar. Pet. Geology*. 97, 78–93. doi:10.1016/j.marpetgeo.2018.06.009

Li, C., Zhou, S., Li, J., Yang, Y., Fu, D., Ma, Y., et al. (2017). Pore Characteristics and Controlling Factors of the Yanchang Formation Mudstone and Shale in the South of Ordos Basin. *Acta Sedimentologica Sinica* 35 (02), 315–329. (in Chinese with English abstract).

Li, T., Jiang, Z., Song, G., Li, Z., Zhu, R., Su, S., et al. (2019). Analysis of Differences in Pore Structure between continental and marine Shale Reservoirs. *Pet. Geology. Recovery Efficiency* 26 (01), 65–71. (in Chinese with English abstract).

Li, Y., Fan, T., Zhang, J., Zhang, J., Wei, X., Hu, X., et al. (2015). Geochemical Changes in the Early Cambrian Interval of the Yangtze Platform, South China: Implications for Hydrothermal Influences and Paleocean Redox Conditions. *J. Asian Earth Sci.* 109, 100–123. doi:10.1016/j.jseaes.2015.05.003

Liang, C., Jiang, Z., Cao, Y., Zhang, J., and Guo, L. (2017). Sedimentary Characteristics and Paleoenvironment of Shale in the Wufeng-Longmaxi Formation, North Guizhou Province, and its Shale Gas Potential. *J. Earth Sci.* 28, 1020–1031. doi:10.1007/s12583-016-0932-x

Liang, C., Jiang, Z., Zhang, C., Guo, L., Yang, Y., and Li, J. (2014). The Shale Characteristics and Shale Gas Exploration Prospects of the Lower Silurian Longmaxi Shale, Sichuan Basin, South China. *J. Nat. Gas Sci. Eng.* 21, 636–648. doi:10.1016/j.jngse.2014.09.034

Liu, G., Jin, Z., Deng, M., Zhai, C., Guan, H., and Zhang, C. (2015). Exploration Potential for Shale Gas in the Upper Permian Longtan Formation in Eastern Sichuan Basin. *Oil Gas Geology*. 36 (03), 481–487. (in Chinese with English abstract).

Liu, J., Yao, Y., Elsworth, D., Liu, D., Cai, Y., and Dong, L. (2017). Vertical Heterogeneity of the Shale Reservoir in the Lower Silurian Longmaxi Formation: Analogy between the Southeastern and Northeastern Sichuan Basin, SW China. *Minerals* 7 (8), 151. doi:10.3390/min7080151

Long, S., Cao, Y., Zhu, J., Zhu, T., and Wang, F. (2016). A Preliminary Study on Prospects for Shale Gas Industry in China and Relevant Issues. *Oil Gas Geology*. 06, 847–853. (in Chinese with English abstract).

Loucks, R. G., Reed, R. M., Ruppel, S. C., and Hammes, U. (2012). Spectrum of Pore Types and Networks in Mudrocks and a Descriptive Classification for Matrix-Related Mudrock Pores. *Bulletin* 96 (6), 1071–1098. doi:10.1306/08171111061

Loucks, R. G., Reed, R. M., Ruppel, S. C., and Jarvie, D. M. (2009). Morphology, Genesis, and Distribution of Nanometer-Scale Pores in Siliceous Mudstones of the Mississippian Barnett Shale. *J. Sediment. Res.* 79 (12), 848–861. doi:10.2110/jsr.2009.092

Lu, X., Li, F., and Watson, A,T. (1995). Adsorption Measurements in Devonian Shales. *Fuel* 74 (4), 599–603. doi:10.1016/0016-2361(95)98364-k

Montgomery, S. L., Jarvie, D. M., Bowker, K. A., and Pollastro, R. M. (2005). Mississippian Barnett Shale, Fort Worth basin, north-central Texas: Gas-Shale Play with Multi-Trillion Cubic Foot Potential. *Bulletin* 89 (2), 155–175. doi:10.1306/09170404042

Nie, H., Jin, Z., Bian, R., and Du, W. (2016). The"source-cap Hydrocarbon-Controlling"enrichment of Shale Gas in Upper Ordovician Wufeng Formation-Lower Silurian Longmaxi Formation of Sichuan Basin and its Periphery. *Acta Petrolei Sinica* 37 (05), 557–571. (in Chinese with English abstract).

Nie, H., Jin, Z., Ma, X., Liu, Z., Lin, T., and Yang, Z. (2017a). Graptolites Zone and Sedimentary Characteristics of Upper Ordovician Wufeng FormationLower Silurian Longmaxi Formation in Sichuan Basin and its Adjacent Areas. *Acta Petrolei Sinica* 38 (02), 160–174. (in Chinese with English abstract).

Nie, H., Ma, X., Yu, C., Ye, X., Bian, R., and Liu, Z. (2017b). Shale Gas Reservoir Characteristics and its Exploration Potential-Analysis on the Lower Jurassic Shale in the Eastern Sichuan Basin. *Oil Gas Geology*. 38 (03), 438–447. (in Chinese with English abstract).

Pollastro, J,B. (2002). Fractured Shale-Gas Systems. *AAPG Bulletion* 86 (11), 1921–1938.

Qiu, X., Liu, C., Mao, G., Deng, Y., Wang, F., and Wang, J. (2015). Major, Trace and Platinum-Group Element Geochemistry of the Upper Triassic Nonmarine Hot Shales in the Ordos basin, Central China. *Appl. Geochem*. 53, 42–52. doi:10.1016/j.apgeochem.2014.11.028

Reed, R,M., and Loucks, R,G. (2007). Imaging Nanoscale Pores in the Mississippian Barnett Shale of the Northern Fort Worth Basin. *AAPG Annu. Convention Abstr*. 16, 115.

Romero-Sarmiento, M.-F., Rouzaud, J.-N., Bernard, S., Deldicque, D., Thomas, M., and Littke, R. (2014). Evolution of Barnett Shale Organic Carbon Structure and Nanostructure with Increasing Maturation. *Org. Geochem*. 71, 7–16. doi:10.1016/j.orggeochem.2014.03.008

Ross, D. J. K., Bustin, R. M., and Bustin, R,M. (2006). Sediment Geochemistry of the Lower Jurassic Gordondale Member, Northeastern British Columbia. *Bull. Can. Pet. Geology*. 54 (4), 337–365. doi:10.2113/gscpgbull.54.4.337

Ross, D. J. K., and Bustin, R. M. (2008). Characterizing the Shale Gas Resource Potential of Devonian-Mississippian Strata in the Western Canada Sedimentary basin: Application of an Integrated Formation Evaluation. *Bulletin* 92 (1), 87–125. doi:10.1306/09040707048

Schettler, P, D., and Parmoly, C, R. (1990). The Measurement of Gas Desorption Isotherms for Devonian Shale. *GRI Devonian Gas Shale Tech. Rev*. 7 (1), 4–9.

Schmitt, M., Fernandes, C. P., Da Cunha Neto, J. A. B., Wolf, F. G., and dos Santos, V. S. S. (2013). Characterization of Pore Systems in Seal Rocks Using Nitrogen Gas Adsorption Combined with Mercury Injection Capillary Pressure Techniques. *Mar. Pet. Geology*. 39 (1), 138–149. doi:10.1016/j.marpetgeo.2012.09.001

Sing, K. S. W., Everett, D, H., Haul, R, A, W., Moscou, L., Pierotti, R, A., Rouquerol, J., et al. (1985). Reporting Physisorption Data for Gas/solid Systems with Special Reference to the Determination of Surface Area and Porosity (Recommendations 1984). *Pure Appl. Chem*. 57 (4), 603–619. doi:10.1351/pac198557040603

Slatt, R. M., and O'Brien, N. R. (2011). Pore Types in the Barnett and Woodford Gas Shales: Contribution to Understanding Gas Storage and Migration Pathways in fine-grained Rocks. *Bulletin* 95 (12), 2017–2030. doi:10.1306/03301110145

Sun, M., Yu, B., Hu, Q., Chen, S., Xia, W., and Ye, R. (2016). Nanoscale Pore Characteristics of the Lower Cambrian Niutitang Formation Shale: a Case Study from Well Yuke #1 in the Southeast of Chongqing, China. *Int. J. Coal Geology*. 154-155, 16–29. doi:10.1016/j.coal.2015.11.015

Tang, X., Jiang, Z., Jiang, S., Cheng, L., and Zhang, Y. (2017). Characteristics and Origin of *In-Situ* Gas Desorption of the Cambrian Shuijingtuo Formation Shale Gas Reservoir in the Sichuan Basin, China. *Fuel* 187, 285–295. doi:10.1016/j.fuel.2016.09.072

Tang, X., Jiang, Z., Jiang, S., Wang, P., and Xiang, C. (2016). Effect of Organic Matter and Maturity on Pore Size Distribution and Gas Storage Capacity in High-Mature to post-mature Shales. *Energy Fuels* 30 (11), 8985–8996. doi:10.1021/acs.energyfuels.6b01499

Tang, X., Jiang, Z., Li, Z., Gao, Z., Bai, Y., Zhao, S., et al. (2015). The Effect of the Variation in Material Composition on the Heterogeneous Pore Structure of High-Maturity Shale of the Silurian Longmaxi Formation in the southeastern

Sichuan Basin, China. *J. Nat. Gas Sci. Eng*. 23, 464–473. doi:10.1016/j.jngse.2015.02.031

Tian, H., Pan, L., Xiao, X., Wilkins, R. W. T., Meng, Z., and Huang, B. (2013). A Preliminary Study on the Pore Characterization of Lower Silurian Black Shales in the Chuandong Thrust Fold Belt, Southwestern China Using Low Pressure N2 Adsorption and FE-SEM Methods. *Mar. Pet. Geology*. 48, 8–19. doi:10.1016/j.marpetgeo.2013.07.008

Tong, C. (1992). Mechanism of Forming Fault-Folded Structure in Sichuan basin. *Nat. Gas Industry* 12 (05), 1–6+6. (in Chinese with English abstract).

Wang, L., and Wang, Q. (2013). Formation Conditions and Explorative Directions of Jurassic Shale Gas in Fuling Sichuan Basin. *J. Northwest University(Natural Sci. Edition)* 43 (05), 757–764. (in Chinese with English abstract).

Wang, P., Jiang, Z., Chen, L., Yin, L., Li, Z., Zhang, C., et al. (2016a). Pore Structure Characterization for the Longmaxi and Niutitang Shales in the Upper Yangtze Platform, South China: Evidence from Focused Ion Beam-He Ion Microscopy, Nano-Computerized Tomography and Gas Adsorption Analysis. *Mar. Pet. Geology*. 77, 1323–1337. doi:10.1016/j.marpetgeo.2016.09.001

Wang, P., Jiang, Z., Ji, W., Zhang, C., Yuan, Y., Chen, L., et al. (2016b). Heterogeneity of Intergranular, Intraparticle and Organic Pores in Longmaxi Shale in Sichuan Basin, South China: Evidence from SEM Digital Images and Fractal and Multifractal Geometries. *Mar. Pet. Geology*. 72, 122–138. doi:10.1016/j.marpetgeo.2016.01.020

Warlick, D. (2006). Gas Shale and CBM Development in North America. *Oil Gas Financial J*. 3 (11), 1–5.

Wei, X., Huang, J., Li, Y., Wang, Q., Liu, R., and Wen, Z. (2014). The Main Factors Controlling the Enrichment and High Production of Daanzhai Member continental Shale Gas in Yuanba Area. *Geology. China* 41 (03), 970–981. (in Chinese with English abstract).

Wu, J., Liang, C., Hu, Z., Yang, R., Xie, J., Wang, R., et al. (2019). Sedimentation Mechanisms and Enrichment of Organic Matter in the Ordovician Wufeng Formation-Silurian Longmaxi Formation in the Sichuan Basin. *Mar. Pet. Geology*. 101, 556–565. doi:10.1016/j.marpetgeo.2018.11.025

Wu, J., Liang, C., Jiang, Z., and Zhang, C. (2018). Shale Reservoir Characterization and Control Factors on Gas Accumulation of the Lower Cambrian Niutitang Shale, Sichuan Basin, South China. *Geol. J*. 54, 1–13. doi:10.1002/gj.3255

Yang Chao, C., Zhang, J., Li, W., Jing, T., Sun, R., Wang, Z., et al. (2014). Microscopic Pore Characteristics of Sha-3 and Sha-4 Shale and Their Accumulation Significance in Liaohe Depression. *Oil Gas Geology*. 35 (02), 286–294. (in Chinese with English abstract).

Yang, C., Zhang, J., Tang, X., Ding, J., Zhao, Q., Dang, W., et al. (2017). Comparative Study on Micro-pore Structure of marine, Terrestrial, and Transitional Shales in Key Areas, China. *Int. J. Coal Geology*. 171, 76–92. doi:10.1016/j.coal.2016.12.001

Yang Feng, F., Ning, Z., and Liu, H. (2014). Fractal Characteristics of Shales from a Shale Gas Reservoir in the Sichuan Basin, China. *Fuel* 115, 378–384. doi:10.1016/j.fuel.2013.07.040

Zhang, K., Jiang, S., Zhao, R., Wang, P., Jia, C., and Song, Y. (2022). Connectivity of Organic Matter Pores in the Lower Silurian Longmaxi Formation Shale, Sichuan Basin, Southern China: Analyses from Helium Ion Microscope and Focused Ion Beam Scanning Electron Microscope. *Geol. J*. 2022, 1–13. doi:10.1002/gj.4387

Zhang, K., Jiang, Z., Yin, L., Gao, Z., Wang, P., Song, Y., et al. (2017). Controlling Functions of Hydrothermal Activity to Shale Gas Content-Taking Lower Cambrian in Xiuwu Basin as an Example. *Mar. Pet. Geology*. 85, 177–193. doi:10.1016/j.marpetgeo.2017.05.012

Zhang, K., Peng, J., Liu, W., Li, B., Xia, Q., Cheng, S., et al. (2020a). The Role of Deep Geofluids in the Enrichment of Sedimentary Organic Matter: a Case Study of the Late Ordovician-Early Silurian in the Upper Yangtze Region and Early Cambrian in the Lower Yangtze Region, south China. *Geofluids* 2020, 8868638. doi:10.1155/2020/8868638

Zhang, K., Peng, J., Wang, X., Jiang, Z., Song, Y., Jiang, L., et al. (2020b). Effect of Organic Maturity on Shale Gas Genesis and Pores Development: A Case Study on marine Shale in the Upper Yangtze Region, South China. *Open Geosciences* 12 (2020), 1617–1629. doi:10.1515/geo-2020-0216

Zhang, T., Ellis, G. S., Ruppel, S. C., Milliken, K., and Yang, R. (2012). Effect of Organic-Matter Type and thermal Maturity on Methane Adsorption in Shale-Gas Systems. *Org. Geochem*. 47, 120–131. doi:10.1016/j.orggeochem.2012.03.012

Zhang, W., Guo, M., and Jiang, Z. (2011). Parameters and Method for Shale Gas Reservoir Evaluation. *Nat. Gas Geosci.* 22 (6), 1093–1099. (in Chinese with English abstract).

Zhang, X., Chen, H., Lin, L., Dai, Y., Lin, K., and Qian, L. (2013). Lacustrine Shell beach Distribution Methods of Seismic Prediction Research-A Study in the Yuanba Area of Daanzhai Section. *Sci. Tech. Eng.* 13 (07), 1723–1728. (in Chinese with English abstract).

Zhao, J., Jin, Z., Hu, Q., Liu, K., Liu, G., Gao, B., et al. (2019). Geological Controls on the Accumulation of Shale Gas: A Case Study of the Early Cambrian Shale in the Upper Yangtze Area. *Mar. Pet. Geology.* 107, 423–437. doi:10.1016/j.marpetgeo.2019.05.014

Zhao, J., Shen, P., Ren, L., and Tan, X. (2017). Quantitative Prediction of Gas Contents in Different Occurrence Tates of Shale Reservoirs: A Case Study of the Jiaoshiba Shale Gasfield in the Sichuan Basin. *Nat. Gas Industry* 37 (04), 27–33. (in Chinese with English abstract).

Zhao, W., Li, J., Yang, T., Wang, S., and Huang, J. (2016). Geological Difference and its Significance Ofmarine Shale Gases in South China. *Pet. Exploration Dev.* 43 (4), 499–510. (in Chinese with English abstract). doi:10.1016/s1876-3804(16)30065-9

Zhou, D., Jiao, F., Guo, X., Guo, T., and Wei, Z. (2013a). Geologic Analysis of Middle-Lower Jurassic Shale Reservoirs in Yuanba Area, Northeastern Sichuan Basin. *Pet. Geology. Exp.* 35 (06), 596–600+656. (in Chinese with English abstract).

Zhou, D., Jiao, F., Guo, X., Guo, T., and Wei, Z. (2013b). Geological Features of the Lower Jurassic Shale Gas Play in Fuling Area, the southeastern Sichuan Basin. *Oil Gas Geology.* 34 (04), 450–454. (in Chinese with English abstract).

Zhu, T., Bao, S., and Wang, F. (2012). Pooling Conditions of Non-marine Shale Gas in the Sichuan Basin and its Exploration and Development prospect. *Nat. Gas Industry* 32 (09), 16–21+126127. (in Chinese with English abstract).

Zou, C., Yang, Z., Cui, J., Zhu, R., Hou, L., Tao, S., et al. (2013). Formation Mechanism,geological Characteristics and Development Strategy of Nonmarine Shale Oil in China. *Pet. Exploration Dev.* 40 (1), 14–26. (in Chinese with English abstract). doi:10.1016/s1876-3804(13)60002-6

Zou, C., Zhu, R., Bai, B., Yang, Z., Wu, S., Su, L., et al. (2011). First Discovery of Nano-Pore Throat in Oil and Gas Reservoir in China and its Scientific Value. *Acta Petrologica Sinica* 27 (6), 1857–1864. (in Chinese with English abstract).